Biosensors

International Edition: DOI: 10.1002/anie.201612020
German Edition: DOI: 10.1002/ange.201612020

Real-Time In Vivo Hepatotoxicity Monitoring through Chromophore-Conjugated Photon-Upconverting Nanoprobes

Juanjuan Peng[+], Animesh Samanta[+], Xiao Zeng, Sanyang Han, Lu Wang, Dongdong Su, Daniel Teh Boon Loong, Nam-Young Kang, Sung-Jin Park, Angelo Homayoun All, Wenxuan Jiang, Lin Yuan,* Xiaogang Liu,* and Young-Tae Chang**

Abstract: *Drug toxicity is a long-standing concern of modern medicine. A typical anti-pain/fever drug paracetamol often causes hepatotoxicity due to peroxynitrite $ONOO^-$. Conventional blood tests fail to offer real-time unambiguous visualization of such hepatotoxicity in vivo. Here we report a luminescent approach to evaluate acute hepatotoxicity in vivo by chromophore-conjugated upconversion nanoparticles. Upon injection, these nanoprobes mainly accumulate in the liver and the luminescence of nanoparticles remains suppressed owing to energy transfer to the chromophore. $ONOO^-$ can readily bleach the chromophore and thus recover the luminescence, the presence of $ONOO^-$ in the liver leads to fast restoring of the near-infrared emission. Taking advantages of the high tissue-penetration capability of near-infrared excitation/emission, these nanoprobes achieve real-time monitoring of hepatotoxicity in living animals, thereby providing a convenient screening strategy for assessing hepatotoxicity of synthetic drugs.*

Drug-induced liver injury is a common concern for the majority of modern medicine.[1] Serum alanine aminotransferase (ALT), an enzyme commonly used as the indicator for liver damage, has been used as a gold standard biomarker for evaluating acute hepatocellular injury.[2] However, taking ALT levels as the standard test cannot accurately reflect the situation of liver necrosis; for example, skeletal muscle injury can also raise the level of ALT in the blood.[3] Preclinical hepatotoxicity screening presents a powerful method to identify the potential hepatotoxic effect of candidate drugs during the drug development process. Paracetamol (acetaminophen or APAP) is a commonly used anti-pain/fever drug. An overdose of APAP can cause severe hepatotoxicity due to reactive nitrogen species (RNS) generated in mitochondria, alone or in combination with other drugs.[4] APAP undergoes enzymatic biotransformation in the liver to generate RNS through a cascade of oxidation reactions,[5,6] which involves the participation of Kupffer cells (macrophages in the liver).[7] It has been proposed that the production RNS is an early sign of hepatotoxicity associated with APAP overdosage. In particular, $ONOO^-$ is recognized as a direct indicator of hepatotoxicity.[8] $ONOO^-$ can lead to rapid cell death by reacting with a wide array of biomolecules, such as proteins, lipids, and nucleic acids.[9] Due to the short half-life of $ONOO^-$ (ref. [10]), it is challenging to detect it in plasma. As such, in situ detection of the RNS at the site of formation is required.

To address this issue, we have developed multilayered lanthanide-doped upconversion nanoparticles (UCNPs) coated with polyethyleneimine (PEI) and cyanine (Cy7) chromophores (abbreviated as Cy7-PEI-UCNPs) as the nanoprobe. Upon reacting with $ONOO^-$, the nanoprobe is designed to generate near-infrared (NIR) emission at 800 nm, which can be used to monitor the APAP-induced drug hepatotoxicity within living small animals (Figure 1 a). In contrast to organic fluorophores, UCNPs possess many intriguing characteristics, such as high photostability, not any auto-luminescence, and high signal-to-noise ratio. There-

[*] Dr. J. Peng[+]
State Key Laboratory of Natural Medicines
School of Basic Medical Sciences and Clinical Pharmacy
China Pharmaceutical University
Nanjing, Jiangsu, 211198 (China)
E-mail: pjj@cpu.edu.cn

Dr. J. Peng,[+] Dr. A. Samanta,[+] Dr. D. Su, Dr. N.-Y. Kang, Dr. S.-J. Park, Prof. Y.-T. Chang
Singapore Bioimaging Consortium, Agency for Science Technology and Research (A* STAR)
138667, Singapore (Singapore)
E-mail: chmcyt@nus.edu.sg

X. Zeng, Dr. S. Han, L. Wang, Prof. L. Yuan, Prof. X. Liu, Prof. Y.-T. Chang
Department of Chemistry, National University of Singapore
117543, Singapore (Singapore)
E-mail: chmlx@nus.edu.sg

Dr. D. T. B. Loong
Singapore Institute of Neurotechnology (SINAPSE)
National University of Singapore
117456, Singapore (Singapore)

Dr. S. Han, Prof. A. H. All, W. Jiang
Department of Orthopedic Surgery, National University of Singapore
119228, Singapore (Singapore)

Prof. A. H. All
Departments of Biomedical Engineering and Neurology
Johns Hopkins University, Baltimore (USA)

Prof. L. Yuan
State Key Laboratory of Chemo/Biosensing and Chemometrics College of Chemistry and Chemical Engineering
Hunan University, Changsha, Hunan, 410082 (China)
E-mail: lyuan@hnu.edu.cn

Prof. X. Liu
Institute of Materials Research and Engineering
Agency for Science Technology and Research (A* STAR)
117602, Singapore (Singapore)

[+] These authors contributed equally to this work.

Supporting information and the ORCID identification number(s) for the author(s) of this article can be found under: http://dx.doi.org/10.1002/anie.201612020.

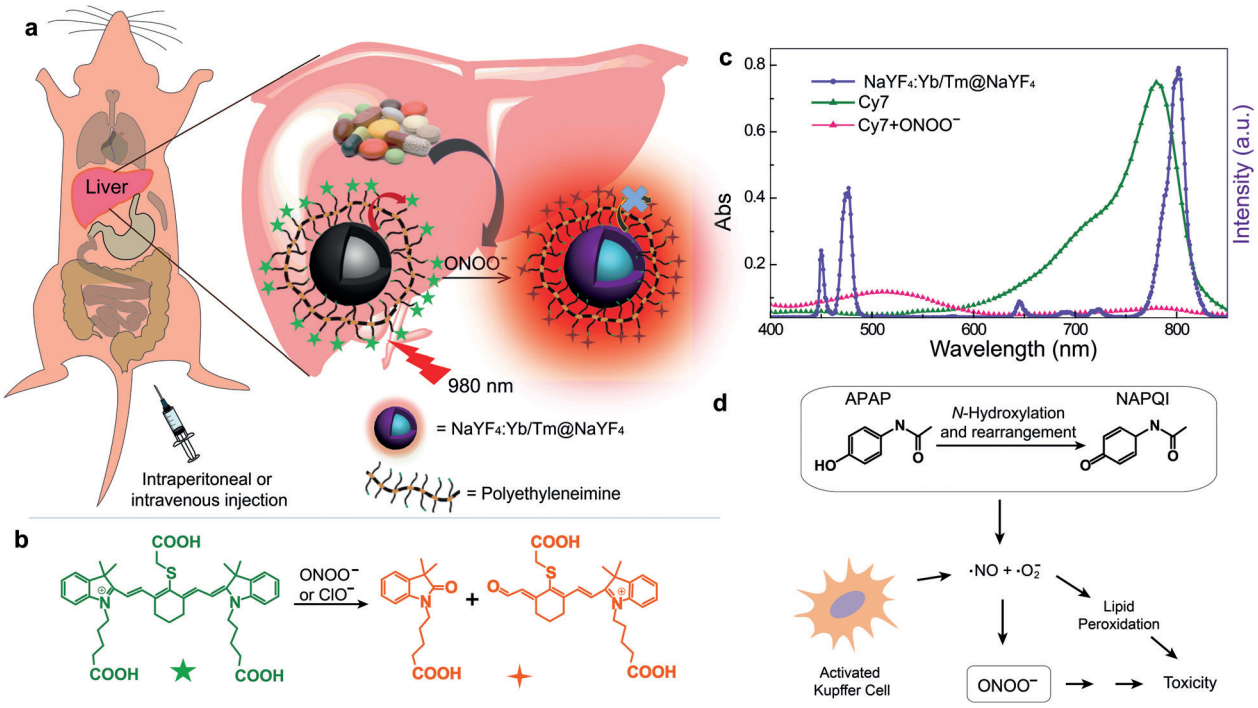

Figure 1. a) Rational design of chromophore-assembled UCNPs for the detection of nitrosative hepatotoxicity in vivo. b) Proposed reaction mechanism for the "turn-on" luminescence by which the energy acceptor Cy7 (marked with green star) degrades after oxidation by $ONOO^-$ or ClO^-. c) UV/Vis spectra of chromophore measured in the absence (green line, 28 μM) and presence (red line, 18 μM) of $ONOO^-$ and upconversion emission spectrum of UCNPs under excitation at 980 nm (purple line). The spectrum was recorded under the excitation of a 980 nm continuous-wave laser at a power of 1 W. d) Mechanism of APAP-induced hepatotoxicity.

fore, UCNPs-based nanoprobes for in vivo imaging and sensing of whole-body animals have recently attracted a great deal of attentions.[11] Till now, a number of UCNPs-based energy transfer systems have been developed to detect various analytes.[12]

Herein, core–shell UCNPs with emission at 800 nm were used as the energy donor and an RNS-responsive NIR absorbing chromophore Cy7 was taken as the energy acceptor (Figure 1 b). In the absence of $ONOO^-$, the Cy7-PEI-UCNPs nanoprobe gives suppressed luminescence at 800 nm due to an efficient energy transfer from the nanoparticle to Cy7. However, once oxidized by RNS, the Cy7 molecule breaks into two parts and is unable to absorb the luminescence emitted by the nanoparticle (Figure 1 c). Therefore, the introduction of RNS leads to turn-on luminescence of UCNPs at 800 nm. As aforementioned, overdosed APAP induces the generation of RNS. Specifically, APAP at a toxic dosage ($>300\ mg\,kg^{-1}$) undergoes *N*-hydroxylation and followed by dehydration through a hepatic cytochrome P450 enzymatic process to form a minor yet significant alkylating metabolite known as NAPQI (*N*-acetyl-*p*-benzoquinone imine) which binds to cellular proteins to induce mitochondrial dysfunction. Moreover, Kupffer cells also participate in the production of reactive nitrogen and oxygen species. During the enzymatic process, $ONOO^-$ has been produced (Figure 1 d) which reacts with biomolecules and eventually causes cell death. Compared to the probes with "turn-off" characteristics, a "turn-on" probe provides a positive signal readout against a dark background with a fine spatial resolution for assessing the drug-induced hepatotoxicity.[13] More importantly, in contrast with the previously reported optical method for the APAP-induced hepatotoxicity assay,[14] which features an excitation at 580 nm and an emission at 820 nm, our UCNPs-based technique involves 980 nm excitation and 800 nm emission, both being located in the NIR spectral region. Such a feature is in favor of biosensing and bioimaging because of its associated low autofluorescence and high penetration depth under in vivo conditions.[15]

To achieve high luminescence intensity for in vivo detection and imaging, core–shell UCNPs ($NaYF_4$:20 % Yb/2 mol % Tm@$NaYF_4$) were synthesized using a layer-by-layer seed-mediated shell growth strategy.[16] Transmission electron microscopy images of the nanoparticles before (see Figure S1a in the Supporting Information) and after (Figure S1b) the shell coating clearly shows an increase in the particle size from 20 to 24 nm. X-ray powder diffraction studies confirm the hexagonal phase of the as-synthesized core–shell nanoparticles (Figure 1 c). Notably, the core–shell design efficiently protects the luminescence of the lanthanide activators from environmental quenching (Figure 2 c,d).[17] To ensure the surface conjugation of Cy7 molecules to the nanoparticles, we first removed stabilizing oleic acid ligands from the nanoparticle by acid treatment, followed by PEI coating and Cy7 coupling. Upon successful conjugation of Cy7 molecules, the colloidal solution turned green and its emission at 800 nm was almost completely quenched (Figure 2 a). We found that the emission lifetime of the as-prepared nanoprobes at 800 nm decreased from 332.4 to

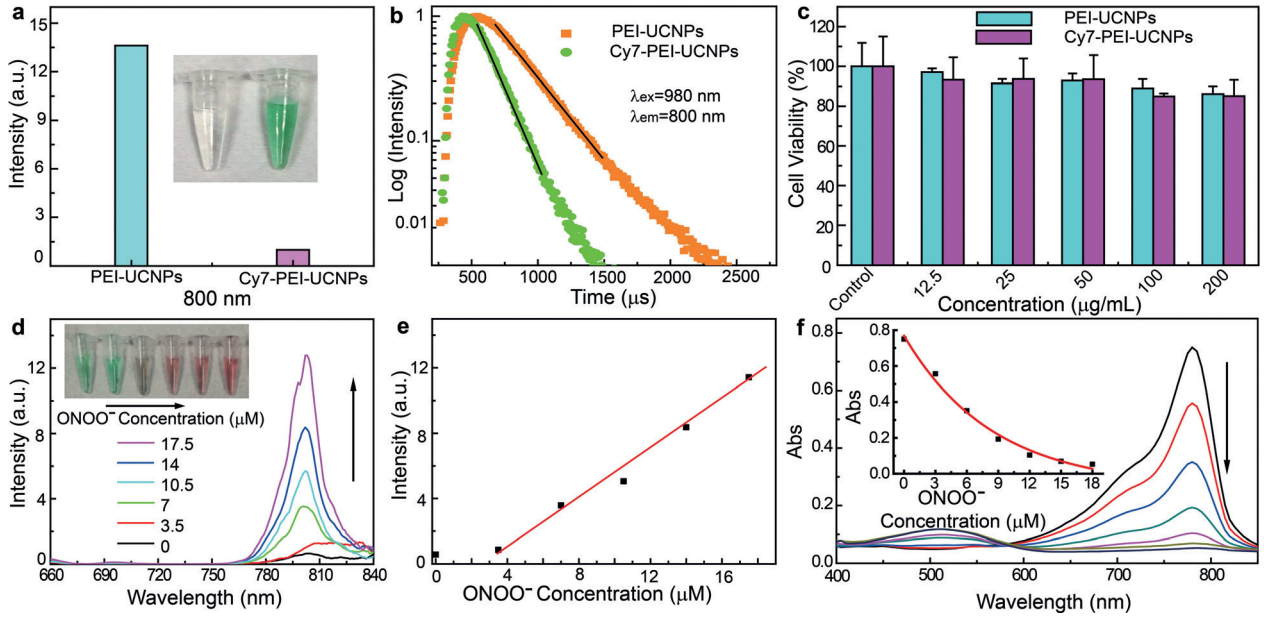

Figure 2. a) Luminescent signals of nanoparticles at 800 nm before and after modification with chromophore dispersed in water. Inset: Color change of the aqueous solution of nanoparticles before and after modification with the chromophore. b) The lifetime of nanoparticles in the absence and presence of dye modification. c) In vitro cell viability of HeLa cells incubated with nanoprobes at different concentrations for 24 h at 37 °C. d) Photoluminescence response of as-developed nanoprobes in aqueous solutions (0.3 mg mL^{-1}) as a function of $ONOO^-$ concentration (0–17.5 μM). The samples were measured under the 980 nm excitation (1 W) immediately after $ONOO^-$ was added. Inset: Color change of the aqueous solution of nanoprobes in the presence of $ONOO^-$. e) The plot of luminescence intensity at 800 nm against the $ONOO^-$ concentration. f) The absorption spectra of the dye (28 μM) upon gradual addition of $ONOO^-$ (from 0 to 18 μM). Inset: Plot of absorption intensity at 780 nm as a function of $ONOO^-$ concentration.

163.1 μs after dye coupling (Figure 2b). The decrease of the average lifetime and intensities indicates that the quenching of luminescence occurs not only through reabsorption but also through Förster resonance energy transfer. The ligand-exchange processing and dye-conjugation step did not induce noticeable changes in the size and morphology of the particles (Figure S2a,b). Infrared spectroscopic and zeta potential characterization further confirm the conjugation of the dye molecules to the surface of the particle (Figure S2c,d).

To furthest quench the luminescence of the nanoparticles, the highest loading amount of Cy7 molecules was adopted. The modification rate was estimated to be 9.8 wt% by spectroscopic absorption analysis (Figure S2e,f), which quenches more than 90% of the upconversion luminescence. The cell viability determined by the methyl thiazolyl tetrazolium assay proved that the as-synthesized nanoprobes have good biocompatibility at different particle concentrations. The survival rates of the Hela cell were higher than 90% in all cases after 24 h of incubation (Figure 2c). The selectivity test proved that the as-developed nanoprobe was only sensitive to the $ONOO^-$ compared with other common ROS/RNS species under the same testing condition. (Figure S3a and 3b) Importantly, the as-developed nanoprobe remains stable when dispersed in biological settings (Figure S3c).

As a proof-of-concept experiment, we explored the utility of the as-synthesized nanoprobes for $ONOO^-$ detection in aqueous solution. $ONOO^-$ of various concentrations ranging from 3.5 to 17.5 μM were spiked into the nanoprobe solution (0.3 mg mL^{-1}). As expected, with increasing $ONOO^-$ concentration, the emission intensity of the nanoprobes at 800 nm was gradually increased (Figure 2d,e), accompanied by the decrease in dye absorption (Figure 2f). To identify the decomposed products of Cy7 on addition of $ONOO^-$, we analyzed the sample with reversed-phase high-performance liquid chromatography and mass spectrometry (Figure S4). These data confirmed that the reaction products have no absorption in the NIR region. In addition, we found that the bleaching response of the Cy7 molecules to $ONOO^-$ could take place within only one second, (Video 1), suggesting the luminescence of developed nanoprobes recovers quickly and is practical for rapid and real-time detection of RNS.

To understand the site-specific targeting of the as-synthesized nanoprobes, the biodistribution of nanoprobes in vivo was studied in BALB\c nude mice. The polyethyleneimine-capped nanoparticles without dye conjugation were chosen. The nanoparticles were intravenously administrated (5 mg mL^{-1}, 100 μL) to mice and their biodistribution was traced by luminescence imagine. Strong luminescence signals were observed near the liver region after injection with the nanoparticles (Figures S5 and S6a). In addition, ex vivo imaging of each organ clearly confirmed that the nanoparticles are accumulated mainly in the liver (Figure S6b,c). We also tracked the biodistribution of the nanoparticles with intraperitoneal injection. After being intraperitoneally injected with nanoparticles for 1 h (100 μL, 5 mg mL^{-1}), the mice were sacrificed to harvest the liver and gastrointestinal system for imaging (Figure S7). The results showed that the nanoparticles can be simultaneously taken up by both the

liver and gastrointestinal system. The liver-targeting property can be attributed to the uptake of the nanoparticles by liver macrophage-Kupffer cells,[18] which are mechanistically important in RNS and superoxide formation. We confirmed the uptake of nanoparticles by Kupffer cells after injection of the nanoparticles by ex vivo microscopy and TEM (Figure S8). Once the APAP is overdosed, the apoptotic hepatocytes will activate the Kupffer cells and trigger the generation of RNS.[4,7] Therefore, our nanoprobes can thus serve as hepatotoxicity sensor through the detection of RNS in the Kupffer cells. It is plausible that the luminescence recovery is due to several factors: disassociation of the dye molecules to the nanoparticles; dye biodegradation, or RNS generation induced by the nanoprobes. To exclude these possibilities, the stability of the nanoprobes was also tested in vivo. In stark contrast with the biodistribution results, after intravenous injection, the luminescence remained undetectable throughout the 6 h timeframe of monitoring (Figure S9). The low background noise over time suggests that these nanoprobes are adequately stable in vivo. By assessing the penetration depth of the visible and NIR emission of UCNPs under 980 nm laser irradiation, we affirm that the NIR (800 nm) light has higher penetration depth than the visible (540 nm and 650 nm), and mitigates auto-fluorescence from the biological sample (Figure S10). Taken together, these results strongly validate the capacity of the as-prepared nanoprobes for RNS detection and imaging in the liver.

As mentioned earlier, an overdose of APAP can result in liver injury through the overproduction of $ONOO^-$. Therefore, APAP-induced hepatotoxicity can be considered as an ideal model to examine the validity of the as-developed nanoprobes for RNS detection in the liver. The selectivity of the nanoprobes depends on the type of chromophore. The specificity of the dye toward $ONOO^-$ under physiological conditions in vitro has been demonstrated previously. In the selectivity test, both $ONOO^-$ and ClO^- were found to lead to dye bleaching in vitro. However, $ONOO^-$ is the main biomarker for APAP-induced hepatotoxicity.[8] Therefore, the luminescence recovery of the nanoprobes can be attributed to $ONOO^-$ in the liver.

To verify the capability of the developed nanoprobes for detection of RNS-induced hepatotoxicity, we carried out intraperitoneal injection of APAP at different concentrations (500, 250 and 0 $mg\,kg^{-1}$) to a series of living mice. After 15 minutes, we injected chromophore-conjugated nanoprobes (5 $mg\,mL^{-1}$, 100 μL) through the tail vein of the mice and then anesthetized them for luminescent imaging at different time intervals (30, 50, and 70 minutes). As shown in Figure 3a, the images captured from the APAP-treated mice showed a remarkable enhancement of luminescent signals in the liver region after particle injection, while a low level of luminescence was observed from the control. Furthermore, the increment of the signals within the liver region is dependent on the dosage of the administrated drug (Figure 3b). Consistent with our ex vivo imaging studies, the signals were mostly obtained from the liver (Figure S11). The emission intensity from the liver of APAP-treated mice was much stronger than that recorded for the control experiment. Consequently, it is conceivable that these nanoprobes are suitable for screening APAP-induced hepatotoxicity in living bodies in response to nitrosative stress in liver.

To verify the possibility of monitoring APAP-induced hepatotoxicity through other administration routes, intraperitoneal injection of the nanoprobes was also employed. Luminescence imaging of the mice injected with APAP at dosages of 250 and 500 $mg\,kg^{-1}$ also showed an obvious signal enhancement after intraperitoneal administration of the nanoprobes (Figures S12 and S13). Ex vivo imaging of each organ showed that both the liver and the gastrointestinal tract have luminescence signals (Figure S14). The luminescence from the gastrointestinal tract is likely due to an increased ROS level.[19] These results demonstrated that the chromophore-conjugated upconversion nanoprobes can be used to detect APAP-induced hepatotoxicity through either intra-

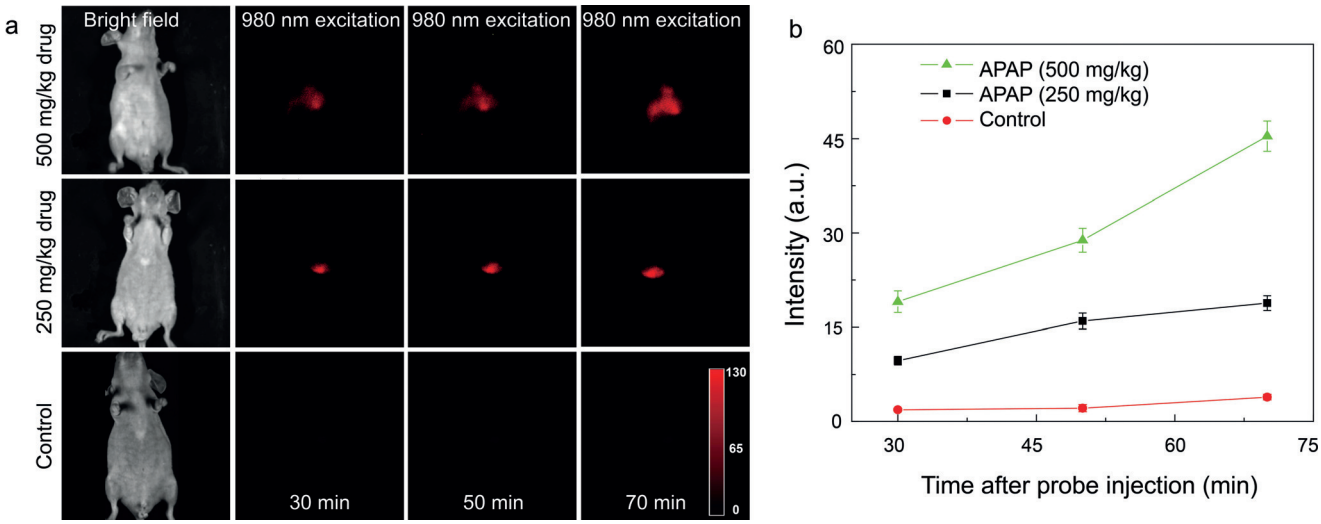

Figure 3. a) Representative images of mice receiving nanoprobes (100 μL, 5 $mg\,mL^{-1}$) pre-treated with 500, 250 $mg\,kg^{-1}$ drug or PBS buffer (control) at a different time point. The images were collected at 790 ± 40 nm upon irradiation at 980 nm. b) The luminescence intensity over time, data were obtained from the liver area of images after the background was subtracted. ($n = 3$ mice per group).

venous or intraperitoneal injection. It should be noted that no marked change in luminescence intensity is observable from the mice injected with a low dosage of APAP (100 mg kg^{-1}) (Figure S15), which is in accordance with the manifestation of APAP-induced hepatotoxicity in mice.[20]

In summary, we have developed a new platform on the basis of "turn-on" luminescence from chromophore-modified upconversion nanoparticles for rapid, sensitive detection of $ONOO^-$ both in vitro and in vivo. Our nanosystem offers a low detection limit down to 0.08 μM (S/N = 3) and a fast in vitro analyte response (less than 1 second). Taking advantage of the unique optical properties of UCNPs, we have also demonstrated our hybrid nanoprobes for in vivo RNS detection in living animal models with APAP-induced hepatotoxicity. Once defined, this UCNPs-based sensing platform may serve as a convenient assay kit to facilitate screening of hepatotoxicity for newly developed drug molecules.

Acknowledgements

This study was supported by A*STAR Joint Council Office (JCO/1231AFG028) and National Natural Science Foundation of China (NSFC/21622504). We would like to thank Mr. Zhigao Yi, Ms. Low Kay En and Ms. Tan Soon Huat for their technical support.

Conflict of interest

The authors declare no conflict of interest.

Keywords: biosensors · fluorescent probes · hepatotoxicity · nanotechnology · paracetamol

How to cite: *Angew. Chem. Int. Ed.* **2017**, *56*, 4165–4169
Angew. Chem. **2017**, *129*, 4229–4233

[1] P. B. Watkins, *Therapy* **2010**, *7*, 367–375.
[2] R. P. L. van Swelm, C. Kramers, R. Masereeuw, F. G. M. Russel, *CNS Drug Rev.* **2014**, *44*, 823–841.
[3] R. A. Nathwani, S. Pais, T. B. Reynolds, N. Kaplowitz, *Hepatology* **2005**, *41*, 380–382.
[4] J. Hinson, D. Roberts, L. James in *Adverse Drug Reactions*, *Vol. 196* (Ed.: J. Uetrecht), Springer, Berlin, **2010**, pp. 369–405.
[5] A. Bertolini, A. Ferrari, A. Ottani, S. Guerzoni, R. Tacchi, S. Leone, *CNS Drug Rev.* **2006**, *12*, 250–275.
[6] J. S. Walsh, G. T. Miwa, *Annu. Rev. Pharmacol. Toxicol.* **2011**, *51*, 145–167.
[7] H. Jaeschke, G. J. Gores, A. I. Cederbaum, J. A. Hinson, D. Pessayre, J. J. Lemasters, *Toxicol. Sci.* **2002**, *65*, 166–176.
[8] C. Cover, A. Mansouri, T. R. Knight, M. L. Bajt, J. J. Lemasters, D. Pessayre, H. Jaeschke, *J. Pharmacol. Exp. Ther.* **2005**, *315*, 879–887.
[9] a) P. Pacher, J. S. Beckman, L. Liaudet, *Physiol. Rev.* **2007**, *87*, 315–424; b) T. Nagano, *J. Clin. Biochem. Nutr.* **2009**, *45*, 111–124.
[10] A. Srivastava, J. L. Maggs, D. J. Antoine, D. P. Williams, D. A. Smith, B. K. Park in *Adverse Drug Reactions*, *Vol. 196* (Ed.: J. Uetrecht), Springer, Berlin, **2010**, pp. 165–194.
[11] a) X. Ai, C. J. H. Ho, J. Aw, A. B. E. Attia, J. Mu, Y. Wang, X. Wang, Y. Wang, X. Liu, H. Chen, M. Gao, X. Chen, E. K. L. Yeow, G. Liu, M. Olivo, B. Xing, *Nat. Commun.* **2016**, *7*, 10432; b) R. Deng, F. Qin, R. Chen, W. Huang, M. Hong, X. Liu, *Nat. Nanotechnol.* **2015**, *10*, 237–242; c) G. Tian, Z. Gu, L. Zhou, W. Yin, X. Liu, L. Yan, S. Jin, W. Ren, G. Xing, S. Li, Y. Zhao, *Adv. Mater.* **2012**, *24*, 1226–1231; d) X. Liu, C.-H. Yan, J. A. Capobianco, *Chem. Soc. Rev.* **2015**, *44*, 1299–1301; e) J. Lai, Y. Zhang, N. Pasquale, K.-B. Lee, *Angew. Chem. Int. Ed.* **2014**, *53*, 14419–14423; *Angew. Chem.* **2014**, *126*, 14647–14651; f) X. Zhu, W. Feng, J. Chang, Y.-W. Tan, J. Li, M. Chen, Y. Sun, F. Li, *Nat. Commun.* **2016**, *7*, 10437; g) S. Han, X. Qin, Z. An, Y. Zhu, L. Liang, Y. Han, W. Huang, X. Liu, *Nat. Commun.* **2016**, *7*, 13059; h) D. Liu, X. Xu, Y. Du, X. Qin, Y. Zhang, C. Ma, S. Wen, W. Ren, E. M. Goldys, J. A. Piper, S. Dou, X. Liu, D. Jin, *Nat. Commun.* **2016**, *7*, 10254; i) C. Drees, A. N. Raj, R. Kurre, K. B. Busch, M. Haase, J. Piehler, *Angew. Chem. Int. Ed.* **2016**, *55*, 11668–11672; *Angew. Chem.* **2016**, *128*, 11840–11845; j) C. Yao, P. Wang, X. Li, X. Hu, J. Hou, L. Wang, F. Zhang, *Adv. Mater.* **2016**, *28*, 9341–9348; k) N. M. Idris, M. K. Gnanasammandhan, J. Zhang, P. C. Ho, R. Mahendran, Y. Zhang, *Nat. Med.* **2012**, *18*, 1580–1585.
[12] a) D. E. Achatz, R. J. Meier, L. H. Fischer, O. S. Wolfbeis, *Angew. Chem. Int. Ed.* **2011**, *50*, 260–263; *Angew. Chem.* **2011**, *123*, 274–277; b) Z. Li, S. Lv, Y. Wang, S. Chen, Z. Liu, *J. Am. Chem. Soc.* **2015**, *137*, 3421–3427; c) J. Shen, L. Zhao, G. Han, *Adv. Drug Delivery Rev.* **2013**, *65*, 744–755; d) J. Peng, C. L. Teoh, X. Zeng, A. Samanta, L. Wang, W. Xu, D. Su, L. Yuan, X. Liu, Y.-T. Chang, *Adv. Funct. Mater.* **2016**, *26*, 191–199.
[13] J. Chan, S. C. Dodani, C. J. Chang, *Nat. Chem.* **2012**, *4*, 973–984.
[14] a) A. J. Shuhendler, K. Pu, L. Cui, J. P. Uetrecht, J. Rao, *Nat. Biotechnol.* **2014**, *32*, 373–380; b) K. Pu, A. J. Shuhendler, J. V. Jokerst, J. Mei, S. S. Gambhir, Z. Bao, J. Rao, *Nat. Nanotechnol.* **2014**, *9*, 233–239.
[15] R. Weissleder, V. Ntziachristos, *Nat. Med.* **2003**, *9*, 123–128.
[16] F. Wang, R. Deng, J. Wang, Q. Wang, Y. Han, H. Zhu, X. Chen, X. Liu, *Nat. Mater.* **2011**, *10*, 968–973.
[17] J. C. Boyer, M. P. Manseau, J. I. Murray, F. C. J. M. van Veggel, *Langmuir* **2010**, *26*, 1157–1164.
[18] J.-K. Park, T. Utsumi, Y.-E. Seo, Y. Deng, A. Satoh, W. M. Saltzman, Y. Iwakiri, *Nanomed. Nanotechnol. Bio. Med.* **2016**, *12*, 1365–1374.
[19] L. A. García Rodríguez, S. Hernández-Díaz, *Arthritis Res. Ther.* **2000**, *3*, 1–4.
[20] M. McGill, H. Jaeschke, *Pharm. Res. Dordr.* **2013**, *30*, 2174–2187.

Manuscript received: December 10, 2016
Revised: January 29, 2017
Final Article published: March 15, 2017

